

IMSc/2001/01/01
MRI-P-010101

Neutrinos from Stellar Collapse: Comparison of signatures in water and heavy water detectors

G. Dutta,

Harish-Chandra Research Institute, Allahabad 211 019, India,

D. Indumathi, M. V. N. Murthy and G. Rajasekaran

The Institute of Mathematical Sciences, Chennai 600 113, India.

(June 20, 2019)

Abstract

Signatures of neutrino and antineutrino signals from stellar collapse in heavy water detectors are contrasted with those in water detectors. The effects of mixing, especially due to the highly dense matter in the supernova core, are studied. The mixing parameters used are those sets allowed by current understanding of available neutrino data: from solar, atmospheric and laboratory neutrino experiments. The dominant charged current interaction on deuteron is very sensitive to some of these sets of allowed mixing parameters. Theoretical uncertainties on supernova neutrino spectra notwithstanding, a combination of supernova measurements with water and heavy water detectors may be able to distinguish many of these mixing possibilities and thus help in ruling out many of them.

I. INTRODUCTION

Neutrinos from stellar collapse have so far been detected only from the supernova SN1987a in the Large Magellanic Cloud [1]. The initial observations of the neutrino and antineutrino events by the Kamiokande [2] and IMB [3] collaborations were the subject of detailed analysis by several authors [4–10] immediately following the event. The analyses confirmed the qualitative features of core collapse and subsequent neutrino emission.

The effect of non-zero neutrino masses and mixing on supernova signals was first analysed in general by Kuo and Pantaleone [11]. Recently, several authors have looked at the possible signatures of neutrinos and antineutrinos from supernova collapse in realistic scenarios. Dighe and Smirnov [12] have looked at the problem of reconstruction of the neutrino mass spectrum in a three-flavour scenario. These authors as also Chiu and Kuo [13] have compared the signatures in the standard mass hierarchy and inverted mass hierarchy. While these papers incorporate the constraints from solar and atmospheric neutrino observations, the important question of the mass limits that may be obtained from the observation of time delay has been analysed by Beacom and Vogel [14,15] and by Choubey and Kar [16] (see also the review by Vogel [17]). For a recent review which also discusses aspects of locating a supernova by its neutrinos in advance of optical observation, see Ref. [18].

In this paper we apply the analysis of neutrinos from stellar collapse presented in Refs. [19,20] to heavy water detectors. We had previously discussed in detail the signatures, in a water Cerenkov detector, of three and four flavours of neutrinos and antineutrinos from stellar collapse. The 4-flavour analysis was motivated by LSND data [21]. The analysis was confined to Type II supernovae (which occur when the initial mass of the star is between 8–20 solar masses). The choices of mixing parameters used were consistent with available data on solar, atmospheric and laboratory neutrino experiments. It turns out that different choices of (allowed) mixing parameters lead to drastically different supernova signals at water detectors. While certain features are common to both the 3- and 4-flavour analyses, there are important differences that may (depending on the mixing parameters) be able to distinguish the number of flavours. We will summarise the salient features of this analysis below.

One possible and dramatic effect of 3-flavour mixing is to produce a sharp increase in the charged current (CC) events involving oxygen targets [22]. These will show up as a marked increase in the number of events in the backward direction with respect to the forward peaked events involving electrons as targets (more than 90% of which lie in a 10° forward cone with respect to the supernova direction for neutrinos with energies $E_\nu \gtrsim 8$ MeV). In the absence of such mixing, there will be only a few events in the backward direction due to CC scattering on oxygen targets. These results hold in a heavy water detector as well; realistically however, there will be fewer such events due to the considerably smaller size of the heavy water detector at the Sudbury Neutrino Observatory (SNO) as compared to the water detector at SuperKamioka (SuperK).

When 4-flavour mixing is considered, the analysis becomes obviously more complex; now, the increase due to oxygen events will be visible only for some of the allowed values of the parameters. Furthermore, there is no set of allowed parameters in both the 3- and 4-flavour cases for which the signals in a water detector will be able to distinguish between adiabatic and non-adiabatic neutrino propagation in the core of the supernova. This is an important

issue since it can place a lower bound on the (13) mixing angle, which is currently bounded by CHOOZ at the upper end in the case of 3-flavour mixing. (The only non-zero value for this angle so far comes from the LSND data which can only be analysed in a 4-flavour frame-work). A zero value for this mixing angle will decouple the two sets of oscillations, $\nu_e \rightarrow \nu_\mu$ and $\nu_\mu \rightarrow \nu_\tau$, and allow for a simple 2-flavour analysis separately of the solar and atmospheric neutrino data. An exactly zero value of this angle will also render irrelevant CP violating phases in the problem.

There are also CC and neutral current (NC) events due to interactions with electrons in water/heavy water. These interactions are the same in both detectors and have already been discussed in detail in the earlier analysis on water detectors [20]. We do not consider them further.

In this paper we focus on the possible signatures of a supernova collapse in a heavy water detector. The question is of practical interest since SNO is operating for more than a year now. It turns out that a combination of measurements in water and heavy water detectors has much better discriminatory power than either of them individually. Hence such observations of supernova neutrinos may be a good signal to rule out some of the currently allowed parameter space in the neutrino mixing angles. (These signals are however not very sensitive to neutrino mass squared differences.)

The most interesting signals to study at a heavy water detector are the mostly isotropic events from CC interactions of both ν_e and $\bar{\nu}_e$ on deuterons. This is the most dominant signal in contrast to the dominant isotropic CC interaction of $\bar{\nu}_e$ alone on free protons in a water detector (all are typically about two orders of magnitude larger than those from oxygen or electron interactions). We will focus mostly on these events in this paper, besides making a few remarks on the NC events on deuteron that can also easily be measured at a heavy water detector. These are therefore the “new” signals in a heavy water detector that would not be observable in (or will be different from) a water detector.

As before the analysis is done assuming the standard mass hierarchy necessitated by the solar and atmospheric neutrino observations [23]. We also impose all the known constraints on the mixing parameters and mass-squared differences including those constraints from laboratory experiments [21,24]. The purpose of the calculation is to see whether different mixing scenarios give significantly different signals in the detector.

In Sect. II we briefly outline the frame-work including the mixing matrix as also matter effects on mixing. We then use this to obtain expressions for the ν_e , $\bar{\nu}_e$ and $\nu_{\mu,\tau}$, $\bar{\nu}_{\mu,\tau}$ fluxes reaching the detector in both 3- and 4-flavour mixing schemes. While discussions may be found in Ref. [19,20] we reproduce the relevant details to keep this paper self-contained. In Sect. III we list the different interaction processes relevant to both water and heavy water detectors and give details of the supernova model used. The allowed values of neutrino mixing parameters (from already existing data) using which the effects of mixing are computed are also listed here. Results are presented showing the effects of mixing both for the spectrum and the integrated number of CC events in Section IV. The NC events in a heavy water detector are also discussed here. All these results are for a (2+2) mass hierarchy scheme in the case of 4 flavour mixing. In Section V, we briefly discuss the other possible scenario, that of the (3 + 1) scheme in 4-flavours. We present a summary and discussions with a passing reference to the supernova SN1987a data in Sect. VI.

II. NEUTRINO MIXING AND MATTER EFFECTS

We briefly review mixing among three and four flavours of neutrinos (or antineutrinos) and compute the neutrino (antineutrino) survival and conversion probabilities. These are given in more detail in Refs. [19,20]. The supernova neutrinos are produced mostly in the core, where the matter density is very high. Hence matter effects on the propagation are important.

The hierarchy of mass eigenstates is shown in Fig. 1. The 3-flavour case is shown in Fig. 1a; there are essentially two scales corresponding to the solution of solar and atmospheric neutrino problems assuming neutrino oscillations. In the case of four flavours (necessitated by the non-zero result of LSND [21]), the analysis is more complicated since there is an additional sterile neutrino. One possible mass hierarchy here is a (2 + 2) scenario [25] as shown in Fig. 1b. The LSND result implies the existence of a mass scale in the range of 0.1 eV² to 1 eV². We choose two doublets separated by this mass scale. The intra-doublet separation in the lower doublet corresponds to the solar neutrino scale $\lesssim 10^{-5}$ eV² and that in the upper one to the atmospheric neutrino scale $\sim 10^{-3}$ eV². Yet another possibility is the so-called (3 + 1) scheme [26,27], where the 3-flavour scheme is extended by adding a heavy sterile neutrino as the heaviest mass eigenstate, with a mass separation from the other three states as required by LSND. We discuss this scheme separately later. In what follows, therefore, 4-flavour mixing always refers to the (2 + 2) scheme.

The mixing matrix, U , which relates the flavour and mass eigenstates in the above scenarios has three angles in the 3-flavour case and six angles in the 4-flavour one. We shall ignore the CP violating phases. Then, the mixing matrix can be parametrised in the case of 3-flavours as,

$$[\nu_e \quad \nu_\mu \quad \nu_\tau]^T = U \times [\nu_1 \quad \nu_2 \quad \nu_3]^T , \quad (1)$$

where T stands for transpose. Here U is parametrised by considering rotations of mass eigenstates taken two at a time:

$$\begin{aligned} U &= U_{23} \times U_{13} \times U_{12} , \\ &= U_\psi \times U_\phi \times U_\omega , \end{aligned} \quad (2)$$

where U_{ij} corresponds to the rotation of mass eigenstates $|i\rangle$ and $|j\rangle$. As is the convention, we denote the mixing angle relevant to the solar neutrino problem by ω and that relevant to the atmospheric neutrino problem by ψ in the case of 3 flavours. The (13) angle is then small, due to the CHOOZ result [24] which translates to the constraint on the (13) mixing angle, $\sin \phi \equiv \epsilon \leq \epsilon_0$, where $\epsilon_0 = 0.16$. In the case of 4-flavours, we choose to work in the (2 + 2) scheme:

$$[\nu_e \quad \nu_s \quad \nu_\mu \quad \nu_\tau]^T = U \times [\nu_1 \quad \nu_2 \quad \nu_3 \quad \nu_4]^T , \quad (3)$$

where the mixing matrix is similarly defined to be,

$$\begin{aligned} U &= U_{34} \times U_{24} \times U_{23} \times U_{14} \times U_{13} \times U_{12} , \\ &= U_\psi \times U_\epsilon \times U_\epsilon \times U_\epsilon \times U_\epsilon \times U_\omega . \end{aligned} \quad (4)$$

Here the (13) and (14) angles are constrained by CHOOZ to be small: $\theta_{13}, \theta_{14} \sim \epsilon \leq \epsilon_0$ [20]. The atmospheric neutrino problem constrains θ_{34} (the equivalent of the angle ψ in the 3-flavour case) to be maximal, when both θ_{23}, θ_{24} become small. We shall assume they are also limited by the same small parameter, ϵ_0 .

The other relevant definition is the chosen mass hierarchy in the problem. We define the mass squared differences as $\delta_{ij} = \mu_i^2 - \mu_j^2$, where i, j run over the number of flavours. Without loss of generality, we can take δ_{21}, δ_{31} (and δ_{41}) to be greater than zero; this defines the standard hierarchy of masses consistent with the range of the mixing angles, as specified above.

A. Matter effects for neutrinos

The most important consequence of the highly dense core matter is to cause Mikheyev, Smirnov and Wolfenstein (MSW) resonances [29] in the neutrino sector. (The chosen mass hierarchy prevents such resonances from occurring in the antineutrino sector). In both the 3- and 4-flavour cases, this causes the electron neutrino to occur essentially as a pure mass state, in fact, as the highest mass eigenstate, as can be seen from the schematic illustration in Fig. 2. Nonadiabatic transitions near the resonances will alter this result, especially in the case of 4-flavours, where there are several level crossings because of the presence of the sterile neutrino. Hence we will discuss the purely adiabatic and the non-adiabatic cases separately.

1. The adiabatic case

We begin with the 3-flavour case. The average transition probability between two flavours α and β is denoted by $P_{\alpha\beta}$ where α, β run over all flavours. It turns out that, independent of other mixing angles and the mass squared differences, the survival probability for the adiabatic case is,

$$P_{ee} = \epsilon^2 , \quad (5)$$

and hence is small. This is sufficient to determine all the relevant fluxes in the 3-flavour case. In the 4-flavour adiabatic case, we again have,

$$P_{ee} = \epsilon^2 , \quad (6)$$

so that the electron neutrino survival probability is flavour independent in the adiabatic case. In addition, we also need to know some other probabilities in order to compute the fluxes at the detector. We have

$$P_{es} = P_{se} = P_{ss} = P_{ee} = \epsilon^2 . \quad (7)$$

2. The non-adiabatic case

Because of the parametrization it is easy to see that non-adiabatic effects in the form of Landau Zener jumps are introduced as a result of the values chosen for ϵ and ω . The value of ϵ determines whether non-adiabatic jumps are induced at the upper resonances while the value of ω determines whether the non-adiabatic jump occurs at the lower resonance. This statement holds both for three and four flavours since in both cases the non-adiabaticity in the upper resonance(s) is controlled by ϵ , apart from mass squared differences.

For a large range of ϵ , allowed by the CHOOZ constraint, the evolution of the electron neutrino is adiabatic. As a result the lower resonance does not come into the picture at all except when ϵ is very close to zero, where the Landau Zener (LZ) jump probability at the upper resonance, P_H , abruptly changes to one [30,11]. This occurs in a very narrow window: for instance, when ϵ changes from 0.02 to 0.01 P_H changes from 0.01 to 0.34. The subsequent discussion is therefore relevant only when ϵ is vanishingly small, $\epsilon \ll 10^{-2}$. (This is not ruled out by the known constraints except LSND).

The LZ transition at the lower resonances is determined by the probability, P_L , which is a function of the mixing angle ω and the mass squared difference δ_{21} . It turns out that P_L is zero unless ω is small, $\sin \omega \lesssim 0.2$ for mass differences in the solar neutrino range. This case corresponds to the extreme non-adiabatic limit. When ω is large, as in the case of the large-angle MSW or the vacuum solution to the solar neutrino problem, non-adiabaticity occurs only at the upper resonance and is therefore partial.

In our calculations we have used the form for P_H and P_L discussed¹ in the appendix of Ref. [19] (see also [30]). Because of the sharpness of the transition at the upper resonance we will set $P_H = 1$ for small enough ϵ and only consider the dependence of the survival probability on the LZ transition at the lower resonance(s).

In the 3-flavour non-adiabatic case the only relevant probability is,

$$P_{ee} = (1 - \epsilon^2)[(1 - P_L) \sin^2 \omega + P_L \cos^2 \omega]. \quad (8)$$

In the non-adiabatic 4-flavour case we have,

$$\begin{aligned} P_{ee} &= (1 - 2\epsilon^2)[(1 - P_L) \sin^2 \omega + P_L \cos^2 \omega], \\ P_{es} &= (1 - 2\epsilon^2)[(1 - P_L) \cos^2 \omega + P_L \sin^2 \omega]. \end{aligned} \quad (9)$$

Since ϵ is small, the flux at the detector is entirely controlled by ω and P_L which is also a function of ω . Note that the sum $P_{ee} + P_{es} = 1 - 2\epsilon^2$ is independent of P_L in 4-flavours. Since $P_{ee} + P_{es} = 1 - P_{e\mu} - P_{e\tau}$, this also indicates that the probability of transition of ν_e into $\nu_{\mu,\tau}$ is small in the non-adiabatic case, in contrast to the adiabatic case where $P_{ee} + P_{es} = 2\epsilon^2$.

¹The Landau Zener transition probability is defined in terms of the adiabaticity parameter, γ , as $P_{LZ} = \exp[-(\pi\gamma F)/2]$, where $F \sim 1$. The final expression for γ given in Appendix B of Ref. [19] should be multiplied by the additional factor $\delta_{31}/60$. However, the numerical calculation in that paper is correct.

B. Matter effects for antineutrinos

Due to our choice of mass hierarchy, the propagation of antineutrinos is always adiabatic (the matter dependent term has the opposite sign as compared to neutrinos).

In the 3-flavour case, we have

$$P_{\bar{e}\bar{e}} = (1 - \epsilon^2) \cos^2 \omega . \quad (10)$$

In the 4-flavour case, we have,

$$\begin{aligned} P_{\bar{e}\bar{e}} &= (1 - 2\epsilon^2) \cos^2 \omega , \\ P_{\bar{e}\bar{s}} &= (1 - 2\epsilon^2) \sin^2 \omega . \end{aligned} \quad (11)$$

Hence, when ω is small, there is very little loss of the $\bar{\nu}_e$ flux into the sterile channel. Also, the sum of $P_{\bar{e}\bar{e}} + P_{\bar{e}\bar{s}}$ behaves similar to the non-adiabatic neutrino propagation case, that is, very little $\bar{\nu}_e$ is converted to $\bar{\nu}_{\mu,\tau}$.

For the NC events, we will also need the following:

$$\begin{aligned} P_{\bar{s}\bar{e}} &= (1 - 2\epsilon^2) \sin^2 \omega + 2\epsilon^2 \sin 2\omega , \\ P_{\bar{s}\bar{s}} &= (1 - 2\epsilon^2) \cos^2 \omega - 2\epsilon^2 \sin 2\omega . \end{aligned} \quad (12)$$

These probabilities can then be used to determine the observed antineutrino fluxes.

C. The neutrino (antineutrino) fluxes at the detector

Following Kuo and Pantaleone [11], we denote the flux distribution, $d\phi_\alpha^0/dE$, of a neutrino (or antineutrino) of flavour α with energy E produced in the core of the supernova by F_α^0 . In particular we use the generic label F_x^0 for flavours other than ν_e and $\bar{\nu}_e$ since

$$F_x^0 = F_{\bar{x}}^0 = F_\mu^0 = F_{\bar{\mu}}^0 = F_\tau^0 = F_{\bar{\tau}}^0 . \quad (13)$$

The ν_e flux on earth is given in terms of the flux of neutrinos produced in the core of the supernova by,

$$\begin{aligned} F_e &= P_{ee}F_e^0 + P_{e\mu}F_\mu^0 + P_{e\tau}F_\tau^0 , \\ &= P_{ee}F_e^0 + (1 - P_{ee})F_x^0 \quad (3\text{-flavours}) , \\ &= P_{ee}F_e^0 + (1 - P_{ee} - P_{es})F_x^0 \quad (4\text{-flavours}) , \end{aligned} \quad (14)$$

where we have made use of the constraint $\sum_\beta P_{\alpha\beta} = 1$. This flux is further reduced by an overall geometric factor of $1/(4\pi d^2)$ for the case of a supernova at a distance d from the earth.

Since the probabilities P_{ee} and P_{es} are known, the ν_e flux can be computed in terms of the original fluxes emitted by the supernova. The result for $\bar{\nu}_e$ is the same, with P_{ee} replaced by $P_{\bar{e}\bar{e}}$, etc. The results are summarised in Tables I and II for the adiabatic neutrino and antineutrino cases, and in Table III for non-adiabatic neutrino propagation. Expressions for the other flavours, needed to compute the NC events, are also given in these tables. For instance,

$$2F_x = F_\mu + F_\tau , \\ = (P_{ee} + P_{es} + P_{se} + P_{ss})F_x^0 + (1 - P_{ee} - P_{se})F_e^0 . \quad (15)$$

A similar expression holds for $F_{\bar{x}}$ with $P_{\alpha\beta}$ replaced by $P_{\bar{\alpha}\bar{\beta}}$.

Typically, models for supernovae predict that the $\bar{\nu}_e$ and ν_x have a hotter spectrum than that of ν_e . This is because the ν_x decouples first since it has only NC interactions with matter and therefore leaves the cooling supernova with the hottest thermal spectrum. The CC interactions of ν_e with matter are larger than those of $\bar{\nu}_e$ and hence ν_e has the coldest spectrum. The model on which this work is based [31] predicts that the average energies of the ν_e , $\bar{\nu}_e$ and ν_x spectra are around 11, 16, and 25 MeV. Keeping this in mind, we observe the following:

1. The ν_e flux is independent of the (12) mixing angles ω in the adiabatic case. Also, it is not very different for 3- and 4-flavours. In both, the observed flux is almost entirely due to the original ν_x flux, and is therefore hotter.
2. There is hardly any mixing of the hotter spectrum into electron antineutrinos in the 4-flavour case; the extent of mixing in 3-flavours depends on the value of ω . For small ω , there is very little change in the electron antineutrino flux.
3. The same result of no mixing from hot spectrum occurs for ν_e as well, in the 4-flavour non-adiabatic case. However, the observed flux can be depleted, depending on the value of P_L . The signal in the 3-flavour case is drastically different. In general, the possibility of LZ transitions makes the analysis more complicated. We will discuss this case numerically later.
4. Finally, while the neutral current (NC) combination, $(\nu_e + 2\nu_x + \bar{\nu}_e + 2\bar{\nu}_x)$, remains unaltered in 3-flavours, there may be actual loss of spectrum into the sterile channel in the 4-flavour case. This should also be a good indicator of the number of flavours involved in the mixing.

Water as well as heavy water detectors will be sensitive to all these aspects of mixing.

In the next section, we will discuss the inputs and constraints, both from supernova models as well as current neutrino experiments. These will then be used to predict numerically supernova event rates in the next section.

III. INPUTS AND CONSTRAINTS

We are interested here in the CC and NC interactions of ν_e and $\bar{\nu}_e$ on deuteron in heavy water. We will also compare the CC interactions to those at a water detector, that is, to $\bar{\nu}_e$ on protons. Interactions on electrons and oxygen nuclei in water and heavy water detectors are the same, and have been discussed in detail in Refs. [19,20].

A. Interaction processes and relevant formulae

Both in water and heavy water detectors, the interaction is mainly of three types:

1. Isotropic events: These are by far the largest fraction of the events, and are due to the CC $\bar{\nu}_e p \rightarrow e^+ n$ interaction in water. In heavy water, there are contributions from both $\bar{\nu}_e d \rightarrow e^+ nn$ and $\nu_e d \rightarrow e^- pp$ CC processes.
2. Forward peaked events: These are due to elastic scatterings of ν_e , $\bar{\nu}_e$, ν_x , $\bar{\nu}_x$ on electron targets in both water and heavy water.
3. Backward peaked events: These arise from CC scattering of ν_e and $\bar{\nu}_e$ on oxygen nuclei in both detectors.

Hence, angular information on the final state electron (e^- or e^+) will allow us to separate out these three types of events. The detailed analysis of signals due to mixing in the forward and backward event samples is given in Ref. [20] for a water Cerenkov detector. These results also hold for a heavy water detector (apart from a scaling factor of 0.9 due to the mass difference between water and heavy water). We will not discuss this further and concentrate on the new results for the isotropic CC events and the NC events. Normally, it may be difficult to separate the isotropic events from the background. However, in this case, since the supernova signal is a short and well defined signal (lasting about 10 secs), it will be possible to detect these events over background (due to solar and other radioactive processes).

The specific CC processes we will consider, for water and heavy water detectors, therefore are

$$\bar{\nu}_e + p \rightarrow e^+ + n , \quad (16)$$

and

$$\begin{aligned} \bar{\nu}_e + d &\rightarrow e^+ + n + n , \\ \nu_e + d &\rightarrow e^- + p + p . \end{aligned} \quad (17)$$

We will also discuss the interesting possibility of observing NC events in a heavy water detector:

$$\begin{aligned} \bar{\nu} + d &\rightarrow \bar{\nu} + n + p , \\ \nu + d &\rightarrow \nu + n + p . \end{aligned} \quad (18)$$

The cross-sections for Eqs. (16), (17) and (18) are well-known [32,33]. The $\bar{\nu}_e p$ cross-section is large in water Cerenkov detectors, being proportional to the square of the antineutrino energy. In terms of total number of events, therefore, water Cerenkov detectors are mostly dominated by $\bar{\nu}_e$ events. In the case of deuteron interactions all cross sections are comparable though the ν_e CC reaction on deuteron has a slightly lower threshold and a somewhat larger cross-section than the CC one on $\bar{\nu}_e$. Also, the $\bar{\nu}_e$ CC cross-section in heavy water is about 4 times smaller than the corresponding one in water due to Pauli suppression. The angular distributions of all these interactions are approximately isotropic in the lab frame. In the

case of the proton target, Eq. (16), there is a slight excess of backward events for energies below 15 MeV, and slight excess in the forward direction at higher energies [34] but the excess in either direction at the relevant energies is limited to a few percent of the total number of events. Since the deuteron is heavier this effect will be even less evident.

1. CC events

Here the recoil electron (positron) is detected. The time integrated event rate, for flavour α and energy E , as a function of the recoil electron (or positron) energy, E_e , is as usual given by,

$$\frac{dN_\alpha^{CC}(E_e)}{dE_e} = \frac{n_t}{4\pi d^2} \sum_b \Delta t_b \int dE F_\alpha(b) \frac{d\sigma^{CC}}{dE_e} . \quad (19)$$

The index b refers to the time interval within which the (original) thermal neutrino spectrum can be assumed to be at a constant temperature T_b . Here n_t refers to the number of scattering targets (of either d or p) that are available in the detector. Also, for these processes, the hadron recoil is so small that we assume $E_e = E - \delta_{IF}$, where δ_{IF} is the mass difference between the initial and final hadrons (including the binding energy). The total number of events from a given flavour of neutrino in a given bin, k , of electron energy (which we choose to be of width 1 MeV) then is

$$N_\alpha^{CC}(k) = \int_k^{k+1} dE_e \frac{dN_\alpha^{CC}}{dE_e} . \quad (20)$$

2. NC events in D_2O

Here, the process is signalled by the break-up of the deuteron and the subsequent 2.2 MeV photon released upon neutron capture. The total number of events is calculated according to

$$N_\alpha^{NC} = \frac{n_t}{4\pi d^2} \sum_b \Delta t_b \int dE F_\alpha(b) \sigma^{NC}(E) . \quad (21)$$

Here again the cross-section is well-known [33].

B. The supernova flux inputs

As in [19,20], we compute the time integrated event rate at prototype 1 Kton water and heavy water detectors from neutrinos emitted by a supernova exploding 10 Kpc away. Results for any other supernova explosion may be obtained by scaling the event rate by the appropriate distance to the supernova and the size of the detector, as shown in Eq. (19). We assume the efficiency and resolution of the detectors to be perfect; this will only slightly enhance the event rates near the detector threshold [20].

We use the luminosity and average energy distributions (as functions of time) for neutrinos of flavour α and energy E as given in Totani et al. [31], based on the numerical modelling of Mayle, Wilson and Schramm [35]. In a short time interval, Δt_b , the temperature can be set to a constant, $T_b(\alpha)$. Then, the neutrino number flux can be described, in this time interval, by a thermal Fermi Dirac distribution,

$$F_\alpha^0(b) = N_0 \frac{\mathcal{L}_b(\alpha)}{T_b^4(\alpha)} \frac{E^2}{(\exp(E/T_b(\alpha)) + 1)}, \quad (22)$$

at a time t after the core bounce. Here b refers to the time-bin, $t = t_0 + b\Delta t$. We set the time of bounce, $t_0 = 0$. The temperature is roughly constant over the entire period of emission (lasting roughly 10 seconds), being given by $T_b(\alpha) = 3.15\langle E \rangle_\alpha$, with the average energy of each flavour, $\langle E \rangle_\alpha = 11, 16, 25$ MeV for $\alpha = \nu_e, \bar{\nu}_e$ and ν_x respectively. The overall normalisation, N_0 , is fixed by requiring that the total energy emitted per unit time equals the luminosity, $\mathcal{L}_b(\alpha)$, in that time interval. The values for $\mathcal{L}_b(\alpha)$ and $T_b(\alpha)$ are taken from Ref. [31]. The total emitted energy in all flavours of neutrinos is about 2.7×10^{53} ergs, which is more or less equally distributed in all flavours. The number of neutrinos emitted in each flavour, however, is not the same since their average energies are different.

With large matter effects present in both the neutrino and antineutrino sector, the validity of the average energies of $\nu_e, \bar{\nu}_e$ and ν_x as 11, 16 and 25 MeV, respectively, which were calculated without mixing, may be questioned. This is especially so because re-scattering effects involve the flavour states which may then equilibrate at different temperatures. We however note that the highly dense matter projects the ν_e and $\bar{\nu}_e$ states as almost pure mass eigenstates. Hence the thermalisation is not affected by effects of mixing. In fact, the effects of mixing are significant only when the resonant densities are reached, when the MSW effect can mix different flavour states. For the parameter values as allowed from current neutrino data, this occurs only at the edge of the neutrinosphere ($R \sim 10^4$ km), and not at the core ($R \sim 50$ km) where most of the neutrinos are produced. This mixing therefore occurs between spectra which are already thermalised to the above-mentioned temperatures. In the case of ν_μ and ν_τ this argument does not go through. In the highly dense core, these are mixtures of more than one mass eigenstate. However, both mix only into each other and scatter through exactly the same processes. Hence their temperatures also remain the same as in the no-mixing case.

C. The mixing parameters

We impose the following known constraints on the mixing matrix in vacuum both for three and four flavour scenarios. Consistent with the CHOOZ constraint, namely $\sin \phi \sim \epsilon \leq \epsilon_0 = 0.16$ which we have imposed at the level of the parametrisation itself, we choose $\epsilon = 0.08$ for the 3-flavour adiabatic case and $\epsilon = 10^{-4} \sim 0$ for the non-adiabatic case. In the case of the 4-flavour scheme, we set $\theta_{13}, \theta_{14}, \theta_{23}, \theta_{24} = \epsilon$.

The constraint from the atmospheric neutrino analysis implies that the relevant angle $\psi (= \theta_{34}) \approx \pi/4$, is near maximal and the relevant mass squared difference is of the order of 10^{-3} eV². Neither of these constraints directly enter our calculations except to determine whether the upper resonance is adiabatic or not depending on the value of ϵ as constrained by the CHOOZ findings. We consider both possibilities here.

The value of the (12) mixing angle, ω , is not yet known. Combined data on solar neutrinos give three possible values [36] :

1. $\sin^2 2\omega = 6.0 \times 10^{-3}, \delta_{21} = 5.4 \times 10^{-6} \text{ eV}^2$ (SMA). The small angle MSW solution.
2. $\sin^2 2\omega = 0.76, \delta_{21} = 1.8 \times 10^{-5} \text{ eV}^2$ (LMA). The large angle MSW solution.
3. $\sin^2 2\omega = 0.96, \delta_{21} = 7.9 \times 10^{-8} \text{ eV}^2$ (LMA-V). The large angle vacuum solution.

This has been slightly modified [37,38] in view of new data from SuperK; however, it remains true, in general, that ω may be small or large, with $\delta_{21} \leq 10^{-5} \text{ eV}^2$.

We will now discuss the results numerically for all these choices.

IV. NUMERICAL RESULTS

The numerical calculations are done by following the evolution of the mass eigenstates through all the resonances including the appropriate jump probabilities when the transition is non-adiabatic (when ϵ is small). Furthermore, the LZ jump at the lower resonances is significant only for the small angle MSW solution for ω .

A. The electron (positron) spectrum

The CC isotropic event rates computed using the above inputs are displayed in Figs. 3–7. The time-integrated event rates per unit electron energy bin (of 1 MeV) are shown as a function of the energy E_e of the detected electron. The solid lines in all the figures refer to the case when there is no mixing and serve as a reference. Results for 3- and 4-flavour mixing are displayed in each of these figures as dotted and dashed lines respectively.

Fig. 3 shows the predictions for the (ω -independent) adiabatic $\nu_e d$ CC interaction when $\epsilon = 0.08$. Mixing enhances the high E_e event rates for both 3- and 4-flavour mixing, which cannot be distinguished here. Furthermore, mixing shifts the peak of the spectrum to higher energies, from 15 MeV to about 28 MeV because of the admixture of the hotter ν_x spectrum and its significantly higher cross-section with deuterium. This high energy shift should be clearly observable.

In Fig. 4 we show the electron spectrum for the non-adiabatic $\nu_e d$ CC interaction when ϵ is small, in fact near zero. The fully non-adiabatic case corresponding to small ω is shown in comparison with that for a larger value of ω in the figure. Here, 3- and 4-flavour mixing give drastically different results, but the small- ϵ scenario is in general not very sensitive to the chosen values of ω .

We would like to point out that the pure ν_e spectrum may not be observable in heavy water. It may be separated out from the total isotropic events if the $\bar{\nu}_e$ spectrum can be reliably estimated from corresponding data at a water detector. However, we will later show that the total number of isotropic events will still be sensitive to the mixing parameters.

In Fig. 5 we show the positron spectrum due to $\bar{\nu}_e d$ CC interactions for two different choices of ω . (Here $\epsilon = 0.08$, but the results are essentially the same even if ϵ is nearly zero since this sector is always adiabatic.) Mixing has appreciable effects only for large ω ; however, mixing does not affect the peak position, unlike in the adiabatic ν_e case.

The total isotropic event rates due to CC $\nu_e d$ and $\bar{\nu}_e d$ processes are shown in Figs. 6 and 7 for the two choices of ϵ . The total isotropic CC events in water, due to $\bar{\nu}_e p$ alone, are also shown for comparison. The most significant difference between the two is that of the adiabatic case with small ω (the lower two panels of Fig. 6 which is independent of the number of flavours. This is because of the enhancement in the ν_e events, independent of ω . At all ω , the peak is at a higher energy than expected from the no-mixing case in heavy water but remains the same for a water detector. This shift may be sufficiently significant and therefore observable, in the adiabatic scenario, for all ω . Finally, the upper two panels of Fig 6 indicate that a significant depletion in the observed isotropic events in water, together with an enhanced number of events in heavy water is an unambiguous signal of 4-flavour mixing with large ω (dashed lines in Fig. 6).

The corresponding results for the total CC events in the non-adiabatic case are shown in Fig. 7. Here there is no significant shift in the spectral peak. Also, the signals in water and heavy water are very similar, with the signals being either enhanced or depleted similarly in both. For instance, the large ω 4-flavour signal shows depletion both in water and heavy water. This may be difficult to distinguish from the no-mixing case if the overall normalisation of the supernova spectrum is uncertain by more than a factor of two. In all cases, the small- ϵ , small- ω scenario also cannot be distinguished from the no-mixing case. Hence the small- ϵ case may be difficult to establish unambiguously, independently of the supernova model inputs.

Keeping in mind that the supernova dynamics may have large uncertainties, we now go on to analyse the total number of events in water and heavy water detectors. These are likely to be less sensitive to the supernova models (although they do depend on the temperature hierarchy for ν_e , $\bar{\nu}_e$ and ν_x) and hence may be more robust signals of mixing.

B. Number of CC events

The predicted time integrated number of events resulting in a scattered electron with energy, $E_e > 5$ MeV (which is a typical threshold for Cerenkov detectors), is shown in Tables IV and V, for the adiabatic and non-adiabatic cases respectively. As before, the number is calculated assuming a supernova explosion at 10 Kpc for a 1 kTon detector. Listed are the mostly isotropic CC events on deuterons in heavy water and free protons in water.

For each target, we have listed the individual contributions from ν_e and $\bar{\nu}_e$ and their total. In particular we tabulate the events for 3- and 4-flavour mixing when ω is both small and large. There are no isotropic events due to ν_e in water.

In Table IV, we show the results for the fully adiabatic case when $\epsilon = 0.08$. Mixing always enhances the ν_e channel by more than a factor of two; hence adiabatic propagation always predicts an enhanced rate of total isotropic events in heavy water even though there is reduction in the $\bar{\nu}_e$ channel for some parameters. In contrast, the total number of events in water may even go down as compared to the no-mixing case, depending on the parameter values.

In Table V, we show similar predictions for the case when $\epsilon \sim 0$ or when the upper resonance becomes fully non-adiabatic. The value of ω then determines whether or not the lower resonance is adiabatic. Recall that the antineutrino propagation is always adiabatic.

Small changes in the antineutrino events between Tables IV and V are due to changes in the value of ϵ . Irrespective of the parameter values, it is seen that there is never any depletion in the 3-flavour case. As in Fig. 7 an interesting scenario occurs when ω is large in the 4-flavour case. Here the total number of events in both ν_e in heavy water and in $\overline{\nu}_e$ in water and heavy water, is reduced by a factor proportional to $\cos^2 \omega$. This is the only scenario where there is depletion in both water and heavy water.

C. Possible discrimination of various models

So far, we have assumed that most of the mixing parameters are known and used the supernova measurement as a potential check for self-consistency of the model parameters. This is because there is still very little known about the supernova neutrino spectrum through observations and hence there is both theoretical and experimental uncertainty about the details of the neutrino spectrum. However, it is still instructive to actually turn the question around and ask, suppose another supernova explosion is observed through its neutrino emission. Will an excess over (or a depletion from) the expected number of events unambiguously determine some of the model mixing parameters? The answer to this question can be obtained from Table VI. It is seen that certain classes of models may be ruled out, depending on the observation. We define the ratio of the total number of events potentially observed from a future supernova (equivalently, the prediction from a given neutrino mixing model) to the expected number of events without mixing (for $E_e > 5$ MeV):

$$R_i = \frac{\text{observed number of events}}{\text{calculated number without mixing}} , \quad (23)$$

where $i = D, H$ refer to heavy water and water detectors respectively. The denominator refers to the the expected number of events (without mixing) as computed from a Monte Carlo simulation that takes into account detector resolution, efficiency, etc., consistent with the detector at which the events were observed. An observation may find $R_i > 1$, $R_i < 1$ or $R_i \sim 1$. The mixing models (with model parameters ϵ and ω , including adiabaticity) consistent with, or predicting such an observation are shown in Table VI. Here the non-adiabaticity, that is, the value of P_L at the lower resonance(s) has been computed assuming a typical value of $\delta_{21} = 10^{-5}$ eV². Water detectors cannot distinguish adiabatic (A) and non-adiabatic (N) scenarios, that is, whether or not ϵ is different from zero, but can distinguish the number of flavours when ω is large (see the last column of Table VI). In D_2O , however, most models predict $R_i > 1$. The only observation of $R_i < 1$ in D_2O occurs for the 4-flavour non-adiabatic case with $\epsilon \sim 0$ and large ω .

On combining data from water and heavy water detectors, an improved discrimination of model parameters is possible, as can be seen from Table VII. Here the possible values of R_H and R_D are listed, along with the possible models that are consistent with such a combined observation. First of all, it is seen that combining the two measurements immediately makes a separation possible between the adiabatic and non-adiabatic cases and hence whether ϵ is different from zero, except in the 3-flavour case with large ω . It should be noted that the $\epsilon, \omega \rightarrow 0$ scenario is unlikely to be distinguished from the no-mixing case. It is also seen that certain combinations of R_D and R_H do not occur for any of the allowed parameters values. For instance a depletion in heavy water is *only* consistent with depletion in water

as well. Any other result in water indicates that the overall normalisation of the spectrum is probably in error. An occurrence of such “forbidden” combinations may therefore can be used as a check on the overall normalisation of the supernova spectrum.

Barring sensitivity to supernova models, the following scenario is best suited to determining the value of ω . (1) There are fewer isotropic events than expected ($R_H < 1$) in a water Cerenkov detector such as SuperK. This reduction factor determines $\cos^2 \omega$. (2) The *same* reduction factor ($R_D < 1$) fits the data from a heavy water detector such as SNO. This can imply that the correct mixing matrix is one with 4 flavours and large ω , with non-adiabatic neutrino propagation. (3) If on the other hand there are enhanced number of events ($R_D > 1$) at the heavy water detector, it clearly indicates adiabatic neutrino propagation. This in turn implies that ϵ is different from zero which has so far been claimed only by LSND. We will add a note on this, with reference to the supernova SN1987a, in the next section.

These qualitative features can be quantified by defining the double ratio,

$$R_{D/H} = \frac{R_D}{R_H}. \quad (24)$$

In practice, it may not be possible to directly take a ratio of the data from water and heavy water detectors since the two measurements will differ in their systematics, apart from such considerations as detector efficiency and resolution. Since $R_i, i = D, H$ are normalised to the theoretical expectancy including these considerations, $R_{D/H}$ is not likely to be sensitive to details of detector design and can thus provide a robust, quantitative indicator of different types of mixing.

This double ratio (where R_i has been calculated as before) has been shown in Fig. 8, as a function of ω . The ratio is plotted for the sum of all CC isotropic events with the cut on the electron energy, $E_e \geq 5$ MeV. The two curves in each figure correspond to two values of ϵ , $\epsilon = 0.08, 10^{-4}$, when the propagation is purely adiabatic (solid lines) or purely non-adiabatic (dashed lines) at the upper resonance. These are the two cases that a water detector is normally not able to resolve. Also shown are dotted lines corresponding to the solutions allowed by the solar neutrino problem: $\sin^2 2\omega = 0.006, 0.76$ and 0.96 . While the 3-flavour mixing case is shown on the left, the 4-flavour result is plotted on the right.

Obviously, a value of unity is expected for the case of no-mixing. We analyse each case in turn.

1. We see from Fig. 8 that the double ratio $R_{D/H}$ is always strictly greater than one for the adiabatic case, independent of ω or the number of flavours, f .
2. Even in the non-adiabatic case, it can be less than one only when $f = 4$. Note however that currently allowed values of ω lead to $R_{D/H} \sim 1$ in the non-adiabatic case. The case $R_{D/H} < 1$ occurs only for intermediate values of ω .
3. For $f = 3$ (left panel of Fig. 8), the double ratio at small ω is different for the adiabatic and non-adiabatic cases, which may therefore be distinguished. However, it may be very difficult to distinguish these two for large values of ω .
4. On the other hand, these two cases are easily distinguished for all ω for $f = 4$ as can be seen from the right panel in the figure.

5. While the double ratio is similar for both $f = 3, 4$ for small ω , $\sin^2 2\omega \leq 0.1$, the number of flavours can be distinguished for larger values of ω , especially in the currently allowed region, only in the adiabatic case.
6. However, as stated before, independent of f , the small ω non-adiabatic solution with $\epsilon \sim 0$ cannot be distinguished from the no-mixing case.

Finally, keeping in mind that a thermal neutrino flux distribution such as the one we have used may overestimate the high energy spectrum, the case $5 \leq E_e$ (MeV) ≤ 40 is shown separately in Fig. 9. Most of the features survive the cuts; hence this ratio is likely to be a stable indicator of mixing.

D. Number of NC events

As is well-known, unlike water detectors, heavy water detectors can directly observe NC events. This is very important in the context of supernova neutrinos since neutrino emission from supernovae is practically the only observable system where neutrinos (and antineutrinos) of all flavours are emitted in roughly equal proportions.

While there is no loss of NC events in the case of 3-flavour mixing, the existence of a fourth flavour will be signalled by loss of NC events into this sterile channel. This can be seen from Tables VIII and IX where the total number of NC events from neutrinos or antineutrinos of all flavours (with $E_\nu > 3$ MeV) is listed for different possible values of ω consistent with the solar neutrino expectation. It is seen that the number of NC events is not very sensitive to the value of ω ; however, from Table VIII it is clear that in the adiabatic case, there is only about 25% depletion with 4-flavour mixing when compared to the no-mixing case. Recall that the CC events are always enhanced by a factor of 1.5–2 for the adiabatic case. Hence the NC events can be used to normalise the supernova spectrum to at least within 25%.

When the upper resonance is non-adiabatic, however, part of the signal gets regenerated, especially for smaller ω . Hence, as Table IX shows, there are roughly the same number of NC events with and without mixing in the non-adiabatic case, independent of the number of flavours. The corresponding CC channel shows severe depletion only when ω is large; otherwise, it is either enhanced, or the same as the no-mixing case. Hence here also the NC events can be used to normalise the supernova spectrum.

V. A NOTE ON THE 4-FLAVOUR (3 + 1) MIXING SCHEME

So far, all results in the 4-flavour analysis referred to the (2 + 2) scheme as shown in Fig. 1b. We briefly discuss results in the (3 + 1) scheme where the mixing matrix is defined through:

$$[\nu_e \quad \nu_\mu \quad \nu_\tau \quad \nu_s]^T = U \times [\nu_1 \quad \nu_2 \quad \nu_3 \quad \nu_4]^T, \quad (25)$$

where the mixing matrix is defined as before:

$$\begin{aligned}
U &= U_{34} \times U_{24} \times U_{23} \times U_{14} \times U_{13} \times U_{12} , \\
&= U_{34} \times U_\epsilon \times U_\psi \times U_\epsilon \times U_\epsilon \times U_\omega .
\end{aligned} \tag{26}$$

Here the (13) and (14) angles are constrained by CHOOZ to be small: $\theta_{13}, \theta_{14} \sim \epsilon \leq \epsilon_0$ [20] as in the (2 + 2) scheme. The atmospheric neutrino problem now constrains θ_{23} (the equivalent of the angle ψ in the 3-flavour case) to be maximal, when θ_{24} becomes small, $\theta_{24} \leq \epsilon_0$. However, the (34) mixing angle is not constrained by any known experimental data.

Since ν_e is produced in the supernova core in essentially the ν_4 mass eigenstate, any non-adiabaticity results in jumps near the upper MSW resonance. The adiabaticity parameter here will be determined by the θ_{14} angle, which is again small, $\theta_{14} = \epsilon$. However, the adiabaticity parameter at the lower resonances depends on the unknown angle θ_{34} and hence we do not comment on the non-adiabatic case here.

The expressions for the fluxes as observed on earth are given in Eqs. 14 and 15 with probabilities $P_{\alpha\beta}$ computed for the (3 + 1) scheme. The relevant probabilities, P_{ee} and P_{es} , for the CC events in the adiabatic case are independent of the unknown angle θ_{34} and are in fact the same in both the (2 + 2) and (3 + 1) schemes. Hence all the results (as shown in Figs. 3, 5, 6) in the adiabatic sector are insensitive to the position of the sterile neutrino in the case of 4-flavours.

In the NC case, we need the probabilities P_{se} and P_{ss} which are different from the (2 + 2) case. Ignoring small terms of order $\mathcal{O}(\epsilon)$, we have,

$$\begin{aligned}
P_{se} &= c_\rho^2 , \\
P_{ss} &= s_\rho^2/2 , \\
P_{\overline{s}e} &= s_\omega^2 s_\rho^2/2 , \\
P_{\overline{s}\overline{s}} &= c_\omega^2 s_\rho^2/2 ,
\end{aligned} \tag{27}$$

where $\rho = \theta_{34}$, the unknown angle in the problem and c_ρ, s_ρ are $\cos \rho$ and $\sin \rho$ respectively.

While these fluxes do depend on θ_{34} , it turns out that the suppression factor in the adiabatic case is again around 75% for both large and small values of ω , independent of the value of θ_{34} . This is because the dominant contribution to the NC sector is from the F_x and $F_{\overline{x}}$ fluxes, as in the (2 + 2) case. These terms are very weakly dependent on the unknown angle θ_{34} . Hence in the NC sector as well, the (adiabatic) (3 + 1) 4-flavour scheme gives the same predictions as the (2 + 2) scheme.

VI. DISCUSSION AND SUMMARY

To summarise, we have contrasted charged current (mostly isotropic) signals from supernova neutrinos (antineutrinos) in water and heavy water detectors. The detailed distribution of events as a function of the scattered electron (positron) energy depends on the number of flavours and the mixing parameters in a complex manner. We have discussed all these cases for the dominant signal from charged current events on deuteron. In particular, Fig. 8 shows the combined sensitivity of water and heavy water detectors to the neutrino mixing parameters for such events. These events are the most interesting feature in a heavy water detector. The signal in this channel is comparable to the antineutrino charged current interaction on protons in water. However, its dependence on the mixing parameters is very

different from that for water. It turns out that a comparison of the signals from water and heavy water detectors can yield important information on not only mixing parameters but also on the number of flavours involved.

By itself, a heavy water detector will also observe events from oxygen and electron scattering. The signals for this are the same as in water detectors and are discussed in Ref. [20]. The main conclusion reached in this case is that mixing typically enhances the CC events due to scattering off oxygen nuclei, which are signalled by an excess of events in the backward direction. Both ν_e and $\bar{\nu}_e$ processes contribute to these events. Elastic scattering off electrons is subdominant; while mixing can enhance the number of events here as well, the total numbers may be insignificant compared to the number of isotropic events. However it may still be possible to observe them since they are sharply peaked in the forward direction with respect to the supernova. Finally, while 3-flavour mixing typically results in an enhanced event rate, 4-flavour mixing can lead to substantial decrease in the number of events, depending on the mixing parameters. While this may not be easy to detect in the case of the oxygen events, the number of isotropic events can substantially decrease, as has also been discussed above.

Before we end, we would like to speculate on the implication of this analysis to the only available data on supernova neutrinos, namely neutrinos from SN1987a [2]. For example, in the no-mixing case, we expect the water Cerenkov detector KII to have observed around 20 events almost all of which are due to $\bar{\nu}_e$. The supernova model that we have used [31] has a $\bar{\nu}_e$ thermal spectrum that is peaked at around 16 MeV; the cross section for the detection of these is proportional to the square of the antineutrino energy. This results in a scattered positron spectrum that is peaked at around 18 MeV.

Although the data set from SN1987a is statistically small, it is curious that the total number of events including the uncertain ones (late signals), is roughly fifty to sixty percent of the total number of events expected. The average energy of the events calculated from the spectrum is close to 16 MeV, albeit with large errors (3 MeV). A look at the RHS of Fig. 6 or 7, where the results for a water detector are plotted, clearly shows that there is exactly one scenario that is consistent with this data set ! This is the one corresponding to 4-flavour mixing, with large ω (assuming that the overall normalisation of the $\bar{\nu}_e$ spectrum has been correctly calculated by the supernova models). Hence, if taken seriously, the KII data seem to indicate that this is the favoured solution. This has the following implication for a future measurement by a heavy water detector: either an excess or a depletion of events alone may be observed. An excess of events over those theoretically expected corresponds to a solution where ϵ is different from zero: the adiabatic solution, as shown in the LHS of Fig. 6 while a depleted signal in heavy water as well indicates a non-adiabatic scenario as in the LHS of Fig. 7. In either case, the mixing parameters will be rather well-determined. Note that such a depletion can also be accounted for in a 4-flavour model that uses an inverted mass hierarchy in the antineutrino sector with a large value of the (12) mixing angle ω . Such a model will be in conflict with the present understanding of the solar neutrino data, unless the vacuum solution is imposed. The inverted mass hierarchy solution is also disfavoured in the 3-flavour analysis [39] unless $\sin^2 \theta_{13} \lesssim 10^{-4}$. The SN1987a data has also been analysed including earth matter effects [40,41]. We reiterate however the intrinsic dangers in using sparse data sets for such analyses. The validity of the above analysis must therefore wait for the next supernova observation.

REFERENCES

- [1] IAU Circular No. 4316, 1987.
- [2] Kamiokande II Collaboration, K. Hirata et al., Phys. Rev. Lett. **58**, 1490 (1987).
- [3] IMB Collaboration, R. M. Bionta et al., Phys. Rev. Lett. **58**, 1494 (1987).
- [4] N. D. Hari Dass, D. Indumathi, A. S. Joshipura and M. V. N. Murthy, Curr. Sci. **56**, 575 (1987).
- [5] J. Arafune and M. Fukugita, Phys. Rev. Lett. **59**, 367 (1987).
- [6] J. N. Bahcall and S. N. Glashow, Nature (London) **326**, 476 (1987).
- [7] K. Sato and H. Suzuki, Phys. Rev. Lett. **58**, 2722 (1987).
- [8] W. D. Arnett and J. L. Rosner, Phys. Rev. Lett. **58**, 1906 (1987).
- [9] E. Kolb, H. Stebbins, and M. Turner, Phys. Rev. D **35**, 3598 (1987).
- [10] R. Cowsik, Phys. Rev. D **37**, 1685 (1988).
- [11] T. K. Kuo and J. Pantaleone, Phys. Rev. D**37**, 298 (1988).
- [12] Amol S. Dighe and Alexei Yu. Smirnov, Phys. Rev. D **62**, 033007 (2000).
- [13] Shao-Hsuan Chiu and T. K. Kuo, Phys. Rev. D **61**, 073015 (2000).
- [14] J. F. Beacom and P. Vogel, Phys. Rev. D **58**, 053010 (1998).
- [15] J. F. Beacom and P. Vogel, Phys. Rev. D **58**, 093012 (1998).
- [16] Sandhya Choubey and Kamales Kar, Phys. Lett. B **479**, 402 (2000).
- [17] Petr Vogel, Invited talk at the 8th Int. Workshop on "Neutrino Telescopes", Venice Feb, 1999, astro-ph/9904338.
- [18] J. F. Beacom, Invited talk at the 23rd Johns Hopkins Workshop on Current Problems in Particle Theory, Neutrinos in the next millennium, Baltimore, June 1999. hep-ph/9909231.
- [19] Gautam Dutta, D. Indumathi, M.V.N. Murthy and G. Rajasekaran, Phys. Rev. D **61**, 013009 (2000).
- [20] Gautam Dutta, D. Indumathi, M.V.N. Murthy and G. Rajasekaran, Phys. Rev. D **62**, 093014 (2000).
- [21] C. Athanassopoulos, LSND Collaboration, Phys. Rev. Lett. **81**, 1774 (1998); Phys. Rev. C **58**, 2489 (1998).
- [22] W. C. Haxton, Phys. Rev. D **36**, 2283 (1987).
- [23] Mohan Narayan, G. Rajasekaran, and S. Uma Sankar, Phys. Rev. D **56**, 437 (1997); Mohan Narayan, M. V. N. Murthy, G. Rajasekaran, and S. Uma Sankar, Phys. Rev. D **53**, 2809 (1996); G. L. Fogli, E. Lisi, A. Marrone, and G. Scioscia, Phys. Rev. D **59**, 117303 (1999); *ibid* 033001; G. L. Fogli, E. Lisi, and D. Montanino, Astropart. Phys. **9**, 119 (1998); G. L. Fogli, E. Lisi, D. Montanino, and G. Scioscia, Phys. Rev. D **56**, 4365 (1997).
- [24] M. Apollonio et al., CHOOZ Collab., Phys. Lett. B **420**, 397 (1998); Phys. Lett. B **466**, 415 (1999) (hep-ex/9907037); Mohan Narayan, S. Uma Sankar, and G. Rajasekaran, Phys. Rev. D **58**, 031301 (1998).
- [25] V. Barger, S. Pakvasa, T.J. Weiler, K. Whisnant, Phys. Rev. D **58**, 093016 (1998) and references therein; V. Barger, P. Langacker, J. Leveille, S. Pakvasa, Phys. Rev. Lett. **45**, 692 (1980).
- [26] E. Ma, G. Rajasekaran, I. Stancu, Phys. Rev. D **61**, 071302 (R) (2000).
- [27] O.L.G. Peres and A. Yu. Smirnov, preprint hep-ph/0011054, 2000.
- [28] Gautam Dutta, D. Indumathi, M.V.N. Murthy and G. Rajasekaran, Talk presented by

DI at the XIV High Energy Physics Symposium, Hyderabad, India, 18–22 Dec, 2000; to be published.

- [29] L. Wolfenstein, Phys. Rev. **D17**, 2369 (1978); S. P. Mikheyev and A. Yu. Smirnov, Sov.J.Nucl.Phys, **42**, 913 (1985); Nuovo Cimento, **C9**, 17(1986).
- [30] S.J. Parke, Phys. Rev. Lett. **57**; See also the review by T. K. Kuo and J. Pantaleone, Rev. Mod. Phys. **61**, 937 (1989).
- [31] T. Totani, K. Sato, H.E. Dalhed, J. R. Wilson, Astrophys. J. **496**, 216 (1998); see also the references in [35] below.
- [32] J. N. Bahcall, *Neutrino Astrophysics*, Cambridge University Press, 1989.
- [33] K. Kubodera and S. Nozawa, Int. J. Mod. Phys. **E3**, 101 (1994).
- [34] P. Vogel and J. F. Beacom, Phys. Rev. D **60**, 053003 (1999).
- [35] A. Burrows and J.M. Lattimer, Astrophys. J. **307**, 107 (1986); R. Mayle, J. R. Wilson and D. N. Schramm, Astrophys. J. **318**, 288 (1987).
- [36] J.N. Bahcall, P.I. Krastev, and A.Yu. Smirnov, Phys. Rev. D **58**, 96016 (1998).
- [37] M.V. Garzelli and C. Giunti, preprint hep-ph/0012247, 2000, talk presented by C. Giunti at NOW 2000, Conca Specchiulla, Otranto, Italy, Sep 2000.
- [38] M.C. Gonzalez-Garcia, M. Maltoni, C. Pena-Garay and J.W.F. Valle, preprint hep-ph/0009350, to appear in Phys. Rev. D.
- [39] H. Minakata and H. Nunokawa, preprint hep-ph/0010240, 2000.
- [40] C. Lunardini, A.Yu. Smirnov, preprint hep-ph/0009356, 2000.
- [41] K. Takahashi, M. Watanabe, and K. Sato, preprint hep-ph/0012354, 2000.

TABLES

No. of flavours	Neutrino flux at detector, F_f
3	$F_e = \epsilon^2 F_e^0 + (1 - \epsilon^2) F_x^0$
4	$F_e = \epsilon^2 F_e^0 + (1 - 2\epsilon^2) F_x^0$
3	$2F_x = (1 + \epsilon^2) F_x^0 + (1 - \epsilon^2) F_e^0$
4	$2F_x = (4\epsilon^2) F_x^0 + (1 - 2\epsilon^2) F_e^0$

TABLE I. $\nu_e, \nu_x = \nu_\mu, \nu_\tau$ fluxes at the detector in the extreme adiabatic limit for 3- and 4-flavour mixing.

No. of flavours	Antineutrino flux at detector, F_f
3	$F_{\bar{e}} = (1 - \epsilon^2) c_\omega^2 F_{\bar{e}}^0 + (s_\omega^2 + \epsilon^2 c_\omega^2) F_x^0$
4	$F_{\bar{e}} = (1 - 2\epsilon^2) c_\omega^2 F_{\bar{e}}^0 + (2\epsilon^2) F_x^0$
3	$2F_{\bar{x}} = (1 + c_\omega^2 - \epsilon^2 c_\omega^2) F_x^0 + (s_\omega^2 + \epsilon^2 c_\omega^2) F_{\bar{e}}^0$
4	$2F_{\bar{x}} = (2 - 4\epsilon^2) F_x^0 + +2\epsilon^2(1 - s_{2\omega}) F_{\bar{e}}^0$

TABLE II. $\bar{\nu}_e, \bar{\nu}_x = \bar{\nu}_\mu, \bar{\nu}_\tau$ fluxes at the detector for 3- and 4-flavour mixing. Here $c_\omega = \cos \omega$, $s_\omega = \sin \omega$.

No. of flavours	Neutrino flux at detector, F_f
3	$F_e = (1 - \epsilon^2)[(1 - P_L)s_\omega^2 + P_L c_\omega^2] F_e^0$ + $[1 - (1 - \epsilon^2)((1 - P_L)s_\omega^2 + P_L c_\omega^2)] F_x^0$
4	$F_e = (1 - 2\epsilon^2)[(1 - P_L)s_\omega^2 + P_L c_\omega^2] F_e^0 + 2\epsilon^2 F_x^0$
3	$2F_x = [1 + (1 - \epsilon^2)((1 - P_L)s_\omega^2 + P_L c_\omega^2)] F_x^0$ + $[1 - (1 - \epsilon^2)((1 - P_L)s_\omega^2 + P_L c_\omega^2)] F_e^0$
4	$2F_x = 2(1 - 2\epsilon^2) F_x^0 + 2\epsilon^2 [1 + (1 - 2P_L)s_{2\omega}] F_e^0$

TABLE III. Neutrino fluxes at the detector when non-adiabatic effects are introduced. While the transition is assumed to be fully non-adiabatic at the upper resonances, it is controlled by the jump probability P_L at the lower resonance. Here c_ω , s_ω and $s_{2\omega}$ refer to $\cos \omega$, $\sin \omega$, and $\sin 2\omega$ respectively.

	Heavy water				Water			
	No Mixing	3-flavours, $s_{2\omega}^2 = 0.96$	4-flavours, $s_{2\omega}^2 = 0.006$	No Mixing	3-flavours, $s_{2\omega}^2 = 0.96$	4-flavours, $s_{2\omega}^2 = 0.006$		
ν_e	72	183	183	181	181	0	0	0
$\bar{\nu}_e$	71	110	71	43	71	290	422	292
Total	143	293	254	224	252	290	422	291

TABLE IV. Total number of events in D_2O from CC events on deuteron due to both ν_e and $\bar{\nu}_e$, producing an electron (or positron) with energy $E_e > 5$ MeV. The results due to no-mixing, and mixing with 3- and 4-flavours in the adiabatic case with $\epsilon = 0.08$ are shown in the three columns. The results with 3- and 4-flavour mixing are shown for two values of ω : ω large ($\sin^2 2\omega = 0.96$) and ω small ($\sin^2 2\omega = 0.006$). For comparison, the CC events due to $\bar{\nu}_e$ on free protons in water is also shown, for the same set of model mixing parameters.

	Heavy water				Water			
	No Mixing	3 flavours, $s_{2\omega}^2 = 0.96$	4 flavours, $s_{2\omega}^2 = 0.006$	No Mixing	3 flavours, $s_{2\omega}^2 = 0.96$	4 flavours, $s_{2\omega}^2 = 0.006$		
ν_e	72	112	88	46	52	0	0	0
$\bar{\nu}_e$	71	110	71	43	71	290	422	291
Total	143	222	159	89	123	290	422	290

TABLE V. The same as Table IV but for a small value of $\epsilon = 10^{-4}$ so that the upper resonance(s) is non-adiabatic.

	Models allowed by the corresponding value of R measured in D_2O		Water	
	$R > 1$	$R < 1$	$R \sim 1$	$R \sim 1$
$R > 1$	$(3\omega_L)_{A,N}, (4\omega_L)_A, (3, 4\omega_S)_A$			$(3\omega_L)_{A,N}$
$R < 1$	$(4\omega_L)_N$			$(4\omega_L)_{A,N}$
$R \sim 1$	$\text{No mix}, (3, 4\omega_S)_N$			$\text{No mix}, (3, 4\omega_S)_{A,N}$

TABLE VI. List of neutrino models which can be discriminated by the D_2O and H_2O detectors. Different values of the mixing angles ω and ϵ give different sets of predictions—more than, less than, and same as the number of events expected without mixing ($R >, <, \sim 1$)—for water and heavy water detectors. The various models are specified by the number of flavours 3 or 4, by the value of ω (ω_L and ω_S refer to $\sin^2 2\omega = 0.96, 0.006$ respectively), and by the suffix A and N referring to adiabatic and non-adiabatic propagation at the upper resonance(s), corresponding to ϵ much larger or much smaller than 10^{-2} respectively.

	Models which are allowed
$R_D > 1; R_H > 1$	$(3\omega_L)_{A,N}$
$R_D > 1; R_H < 1$	$(4\omega_L)_A$
$R_D > 1; R_H \sim 1$	$(3, 4\omega_S)_A$
$R_D < 1; R_H > 1$	None
$R_D < 1; R_H < 1$	$(4\omega_L)_N$
$R_D < 1; R_H \sim 1$	None
$R_D \sim 1; R_H > 1$	None
$R_D \sim 1; R_H < 1$	None
$R_D \sim 1; R_H \sim 1$	No mixing, $(3, 4\omega_S)_N$

TABLE VII. Combined predictions from supernovae signals in water and heavy water and corresponding models with 3 and 4 flavour mixing that are consistent with them. By “None” we mean none of the models of mixing that we have considered here. The notation is the same as in the earlier table with the ratios R_D and R_H referring to heavy water and water respectively.

$\sin^2 2\omega$	Number of events with			$R_{4/0}$
	No mixing	3-flavours	4-flavours	
0.960	374	374	274	0.73
0.760	374	374	281	0.75
0.006	374	374	293	0.78

TABLE VIII. NC events with $E_\nu > 3$ MeV for different values of ω in the adiabatic case when $\epsilon = 0.08$. While the 3-flavour case is identical to the no-mixing case, as expected, the 4-flavour case shows a depletion in events due to loss into the sterile channel. The ratio of the 4-flavour to the no-mixing (or 3-flavour) case is shown in the last column.

$\sin^2 2\omega$	Number of events with			$R_{4/0}$
	No mixing	3-flavours	4-flavours	
0.960	374	374	343	0.92
0.760	374	374	343	0.92
0.006	374	374	364	0.97

TABLE IX. The same as Table VIII, with $\epsilon \sim 0$ so that the upper resonance is non-adiabatic.

FIGURES

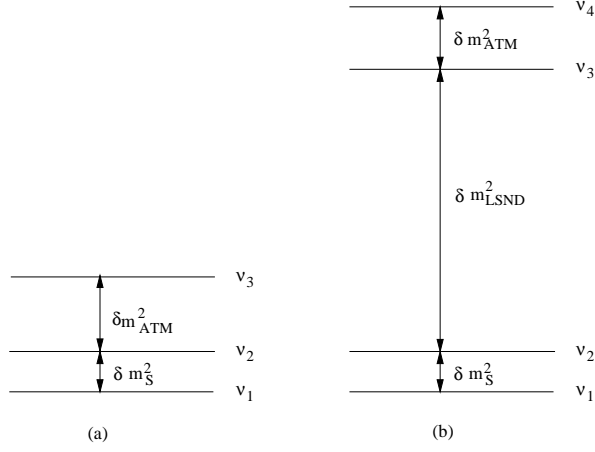


FIG. 1. The vacuum mass square differences in the 3 and 4 flavour schemes. In the 4-flavour scheme, ν_e and ν_s are predominantly mixed states of ν_1 and ν_2 while ν_μ and ν_τ are that of ν_3 and ν_4 (2+2 scheme). The mixing between the lower and upper doublets has been chosen to be very small. Here S, ATM AND LSND stand for the solar, atmospheric and LSND mass squared differences respectively.

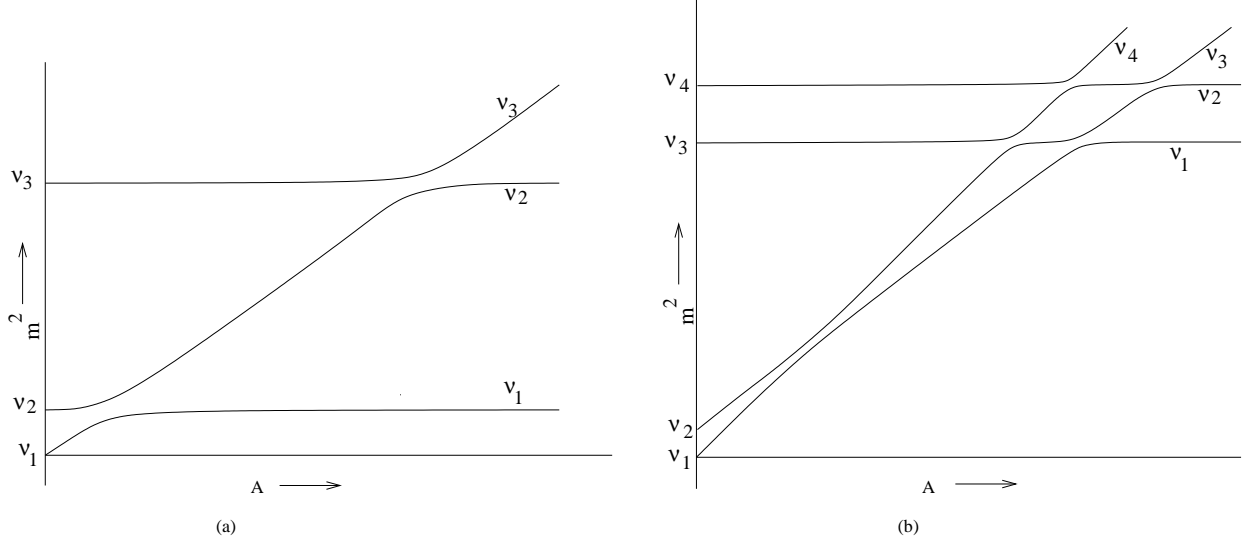


FIG. 2. Schematic drawing showing mass squares as functions of matter density in the 3 and 4 flavour schemes. Resonances occur at two different regions of matter density, the lower one at $\approx \delta m_S^2$. In the 4-flavour case the upper resonances consist of four close-lying resonances determined by δm_{LSND}^2 .

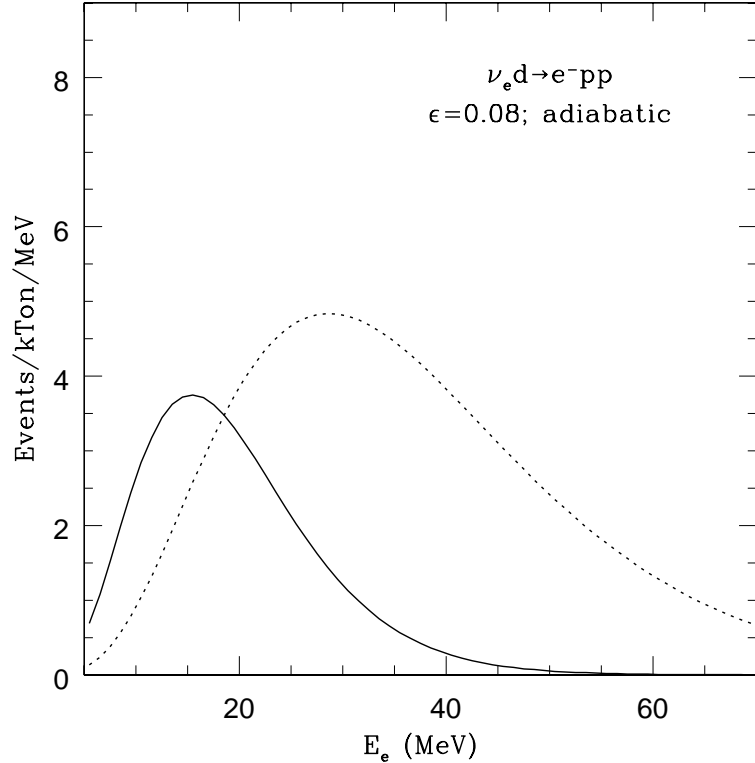


FIG. 3. $\nu_e d$ event rates as a function of the scattered electron energy E_e , when the upper resonance is completely adiabatic. The solid line represents the no-mixing case. The dotted line is due to the effects of either 3- or 4-flavour mixing, which cannot be distinguished here.

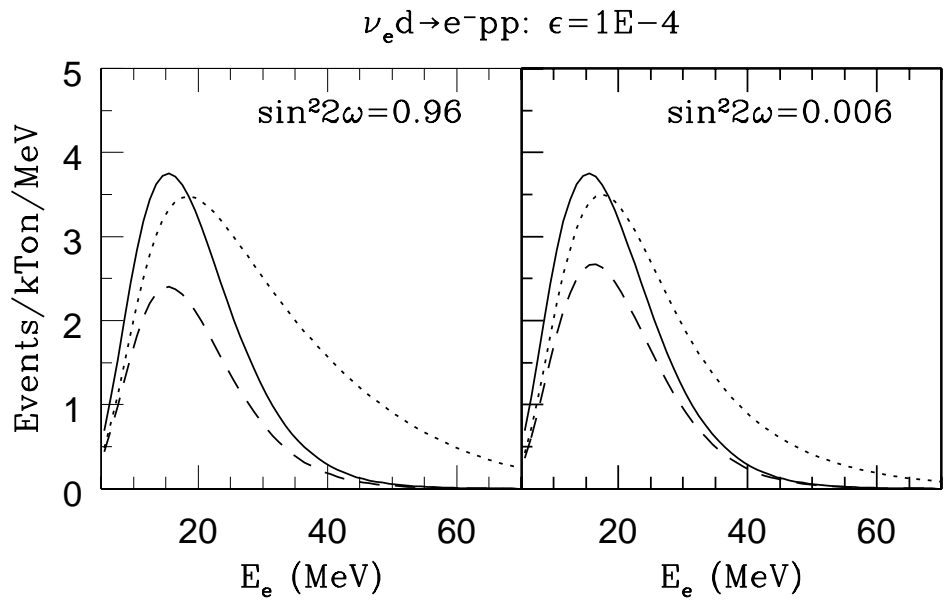


FIG. 4. $\nu_e d$ event rates when the upper resonance is completely non-adiabatic. The solid lines represent the no-mixing case. The dotted and dashed lines are due to the effects of 3- and 4-flavour mixing. Results are shown for two different values of ω .

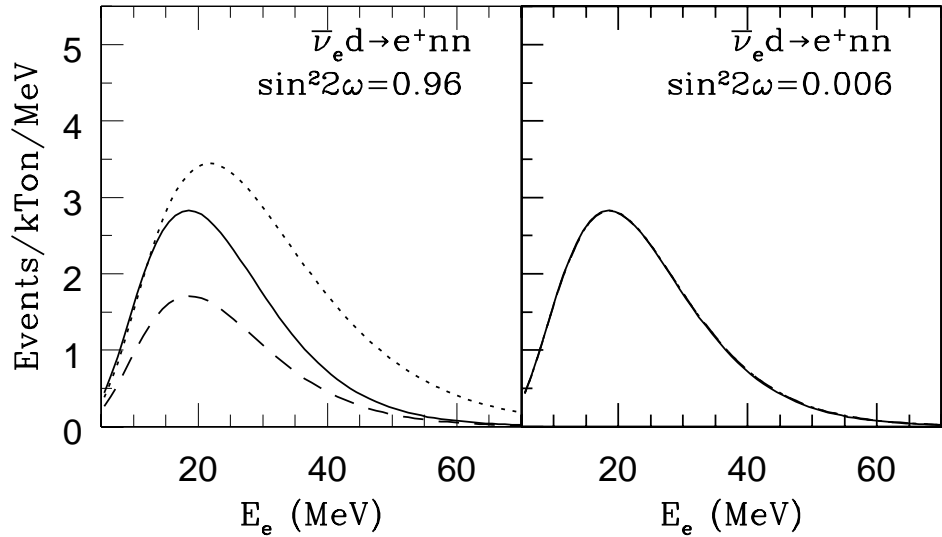


FIG. 5. $\bar{\nu}_e d$ event rates are shown as a function of positron energy, E_e . The solid lines represent the no-mixing case. The dotted and dashed lines are due to the effects of 3- and 4-flavour mixing. Results for two different values of ω are shown.

Total isotropic events, adiabatic case: $\epsilon=0.08$

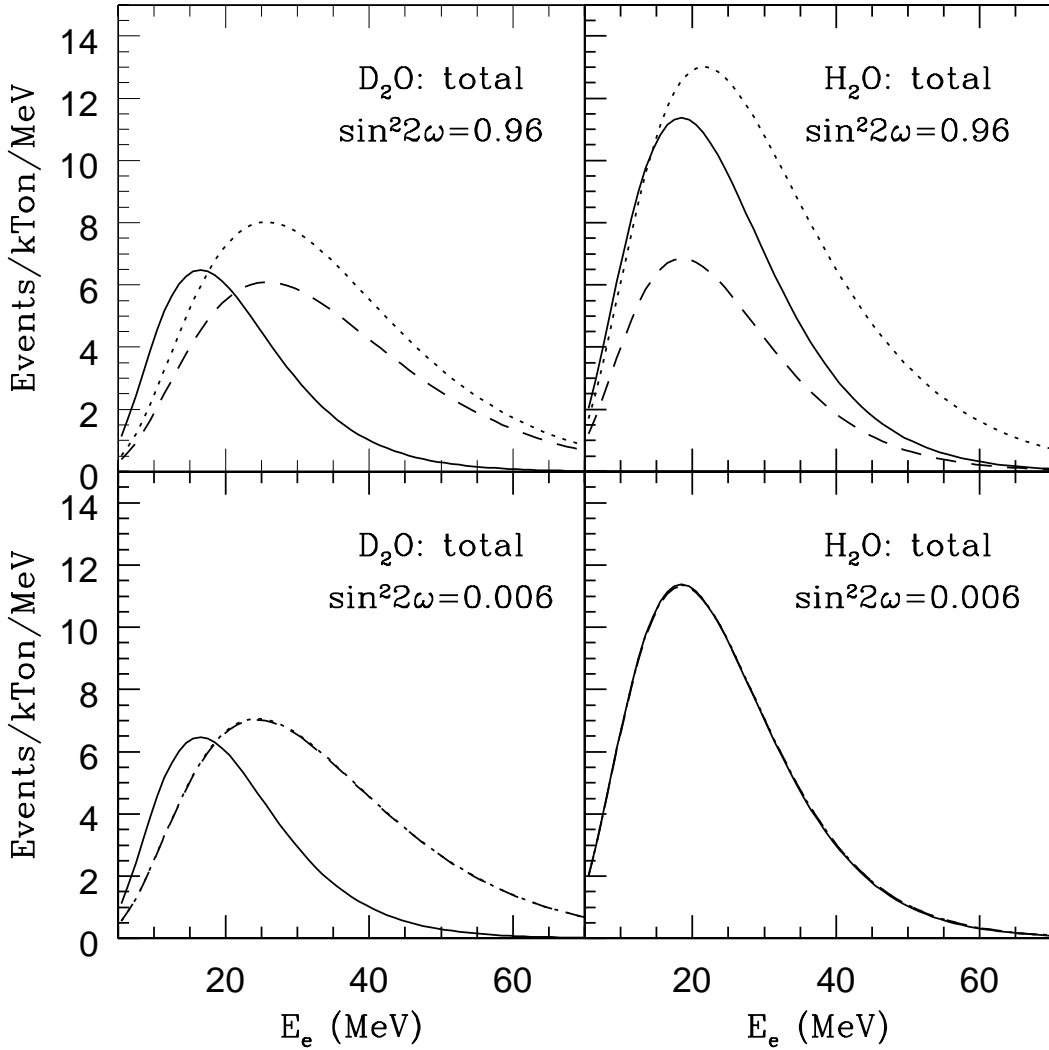


FIG. 6. Total isotropic event rates (from ν_e and $\bar{\nu}_e$) are shown as a function of the electron/positron energy, E_e , for two different values of ω , and for $\epsilon = 0.08$ so that the propagation is fully adiabatic. The dotted and dashed lines are due to the effects of 3- and 4-flavour mixing. Results from a 1 KTon water detector (from $\bar{\nu}_e$ alone) are shown on the right, for comparison.

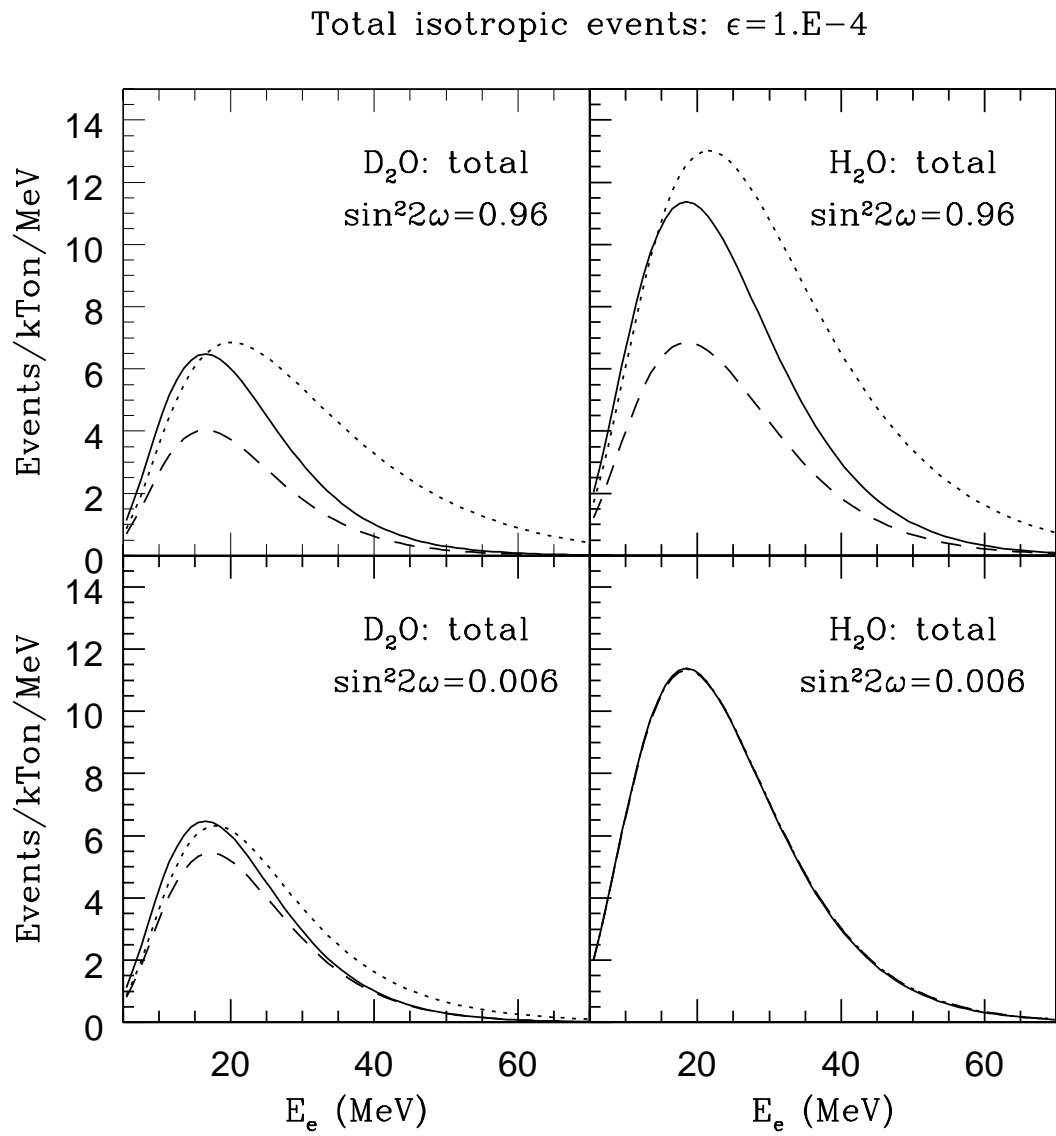


FIG. 7. Same as Fig. 6 but for $\epsilon \sim 0$ so that non-adiabatic effects are included.

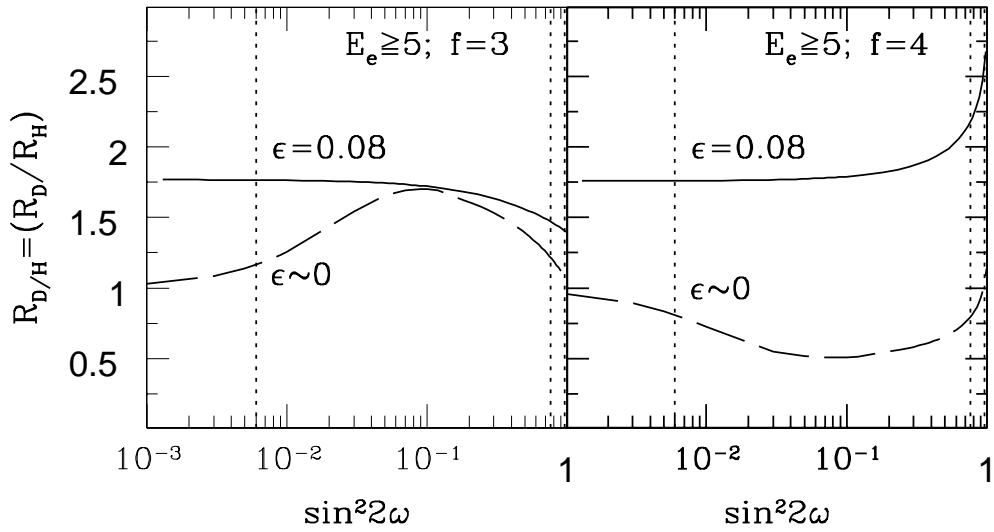


FIG. 8. The double ratio $R_{D/H}$ of the ratio of the total events observed with $E_e \geq 5$ MeV, from a future supernova explosion to that expected, in a heavy water and a water detector, shown as a function of the (12) mixing angle ω . Solid and dashed lines correspond to adiabatic ($\epsilon = 0.08$) and non-adiabatic ($\epsilon \sim 0$) neutrino propagation at the upper resonance. The case for 3-flavour mixing is shown on the left and that for 4-flavours on the right. The vertical dotted lines indicate the currently favoured values of $\sin^2 2\omega$ according to solar neutrino analysis.

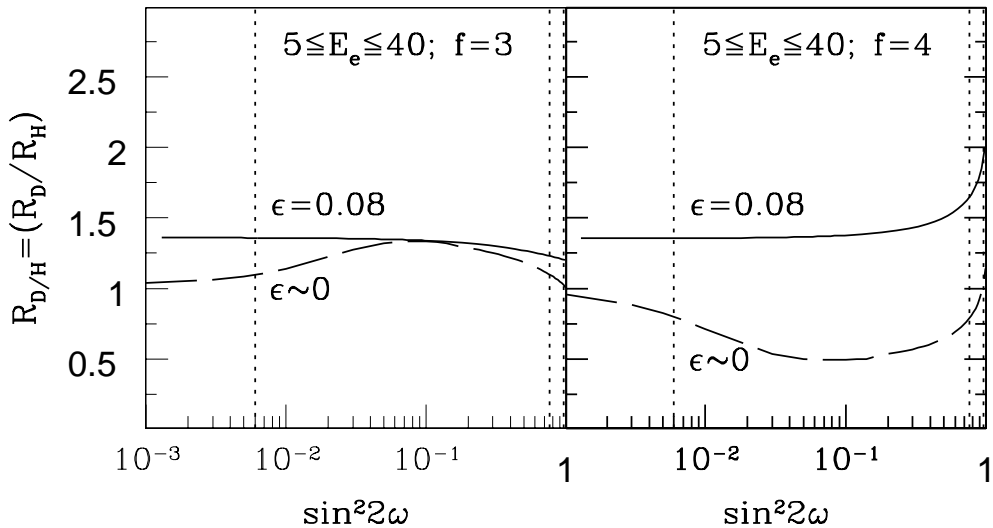


FIG. 9. The same as fig. 8, with a high energy cut on the electrons, $3 < E_e < 40$ MeV, to decrease sensitivity to the more model-dependent high energy tail of the neutrino spectrum.